

Ly α Driven Outflows Around Star Forming Galaxies

Mark Dijkstra^{*} & Abraham Loeb[†]

Harvard-Smithsonian Center for Astrophysics, 60 Garden Street, Cambridge, MA 02138, USA

11 September 2008

ABSTRACT

We present accurate Monte-Carlo calculations of Ly α radiation pressure in a range of models which represent galaxies during various epochs of our Universe. We show that the radiation force that Ly α photons exert on hydrogen gas in the neutral intergalactic medium (IGM), that surrounds minihalos that host the first stars, may exceed gravity by orders of magnitude and drive supersonic winds. Ly α radiation pressure may also dominate over gravity in the neutral IGM that surrounds the HII regions produced by the first galaxies. However, the radiation force is likely too weak to result in supersonic outflows in this case. Furthermore, we show that Ly α radiation pressure may drive outflows in the interstellar medium of star forming galaxies that reach hundreds of km s⁻¹. This mechanism could also operate at lower redshifts $z \lesssim 6$, and may have already been indirectly detected in the spectral line shape of observed Ly α emission lines.

Key words: cosmology: theory–galaxies: high redshift–radiation mechanisms: general–radiative transfer–ISM: bubbles

1 INTRODUCTION

HII regions around massive stars convert a significant fraction of the total bolometric luminosity of young galaxies into Ly α line emission (Partridge & Peebles 1967; Schaerer 2003). This Ly α radiation can exert a large force on surrounding neutral gas, as the Ly α transition has a cross-section that is ~ 7 orders of magnitude larger than the Thomson cross-section, when averaged over a frequency band as wide as the resonance frequency itself (e.g. Loeb 2001). Not surprisingly, the impact of Ly α radiation pressure on the formation of galaxies has been discussed extensively (e.g Cox 1985; Elitzur & Ferland 1986; Bithell 1990; Haehnelt 1995; Oh & Haiman 2002; McKee & Tan 2008), but the intricacies of Ly α radiative transfer in 3D complicated an accurate numerical treatment of its dynamical effect on the gas. Nevertheless, an approximate estimate can be obtained from simple energy considerations as shown below.

Consider a self-gravitating gas cloud of total (baryons + dark matter) mass M and radius R that contains a central Ly α source. The gravitational binding energy of the baryons inside the cloud, $E_B \sim \Omega_b GM^2/(\Omega_m R)$, can be compared to the total energy in the Ly α radiation field inside the cloud, $E_\alpha = L_\alpha \times t_{\text{trap}}$. Here, L_α is the Ly α luminosity of the central source (in erg s⁻¹), and t_{trap} is the typical trapping time of Ly α photons in the cloud owing to

scattering on hydrogen atoms. The Ly α radiation pressure would unbind the baryonic gas from the cloud if $E_\alpha > E_B$, i.e. $L_\alpha > \Omega_b GM^2/(\Omega_m R t_{\text{trap}})$ (e.g. Cox 1985; Bithell 1990; Oh & Haiman 2002). In this approach, t_{trap} is one of the key parameters in setting the Ly α radiation pressure. Calculations by Adams (1975) imply that $t_{\text{trap}} \sim 15 t_{\text{light}}$ for $3 \lesssim \log \tau_0 \lesssim 5.5$, and $t_{\text{trap}} \sim 15(\tau_0/10^{5.5})^{1/3} t_{\text{light}}$ otherwise, for a static, uniform, infinite slab of material (also see Fig 1 of Bonilha et al. 1979). Here τ_0 is the line center optical depth from the center to the edge of the slab, and t_{light} is the light crossing time if the medium were transparent (i.e. $t_{\text{light}} = R/c$ in the case of the cloud described above). Note however, that the precise value of t_{trap} depends on other factors including for example, the gas distribution (clumpiness and geometry), the velocity distribution of the gas, and the dust content of the cloud (Bonilha et al. 1979). The Ly α radiation pressure becomes comparable to gravity when

$$L_{\alpha,41} = 1.0 \left(\frac{M}{10^8 M_\odot} \right)^{4/3} \left(\frac{16}{1+z} \right)^2 \left(\frac{15 t_{\text{light}}}{t_{\text{trap}}} \right), \quad (1)$$

where $L_\alpha = L_{\alpha,41} \times 10^{41}$ erg s⁻¹, and where we have substituted the virial radius of a galaxy mass M , $R_{\text{vir}} = 0.97 \text{ kpc} \times (M/10^8 M_\odot)^{1/3} (1+z/16)^{-1}$, for R (Eq. 24 of Barkana & Loeb 2001). For comparison, a star forming galaxy can generate a Ly α luminosity of $L_\alpha = (10^{42} - 10^{43}) \times (\text{SFR}/M_\odot \text{ yr}^{-1}) \text{ erg s}^{-1}$, where the precise conversion factor depends on the gas metallicity and the stellar initial mass function (e.g. Schaerer 2003). Therefore, a star formation rate of merely $\text{SFR} \gtrsim 0.01 - 0.1 M_\odot \text{ yr}^{-1}$ is needed to gener-

^{*} E-mail: mdijkstr@cfa.harvard.edu

[†] E-mail: aloeb@cfa.harvard.edu

ate a Ly α luminosity that is capable of unbinding gas from a halo of mass $10^8 - 10^9 M_\odot$.

Halos of $\lesssim 10^9 M_\odot$ are very common at $z \gtrsim 6$, and have a sufficiently large reservoir of baryons to sustain the above-mentioned star formation rates for a prolonged time. In this paper we provide a more detailed investigation of the magnitude of Ly α radiation pressure in the environment of high-redshift star forming galaxies. In particular, we use a Ly α Monte-Carlo radiative transfer code (Dijkstra et al. 2006) to compute Ly α radiation pressure in a wider range of models. Our treatment of radiative transfer and our focus on the environment of high-redshift star forming galaxies, distinguish this paper from previous work. We will show that the radiation force exerted by Ly α photons on neutral hydrogen gas can exceed the gravitational force that binds the gas to its host galaxy by orders of magnitude, and may drive supersonic outflows of neutral gas both in the intergalactic and the interstellar medium.

The outline of this paper is as follows. In § 2 we describe how Ly α radiation pressure is computed in the Monte-Carlo radiative transfer code, and show the tests that are performed to test the accuracy of the code. In § 3, we present our numerical results. Finally, § 4 summarizes the implications of our work and our main conclusions. The cosmological parameter values used throughout our discussion are $(\Omega_m, \Omega_\Lambda, \Omega_b, h) = (0.27, 0.73, 0.042, 0.70)$ (Komatsu et al. 2008).

2 LY α RADIATION PRESSURE

The force F_{rad} experienced by an atom in a direction \mathbf{n} is related to the flux through a plane normal to \mathbf{n} ,

$$F_{\text{rad}} = \frac{4\pi}{c} \int d\nu \sigma(\nu) H(\nu), \quad (2)$$

where $\sigma(\nu)$ is the Ly α absorption cross-section at frequency ν . The specific flux is given by $H(\nu) = \frac{1}{2} \int d\mu \mu I(\mu, \nu)$, where $I(\nu, \mu)$ is the specific intensity of the radiation field (see, e.g. Eq. 1.113 in Rybicki & Lightman 1979), and $\mu = \mathbf{n} \cdot \mathbf{k}$ in which \mathbf{k} denotes the propagation direction of the radiation (i.e. $\mu = 1$ for radiation propagating perpendicular to the plane).

The specific intensity obeys the radiative transfer equation, which reads (in spherical coordinates)

$$\mu \frac{\partial I}{\partial r} + \frac{(1 - \mu^2)}{r} \frac{\partial I}{\partial \mu} = \chi_\nu (J - I) + S_\nu(r), \quad (3)$$

where in this equation $\mu \equiv \mathbf{r} \cdot \mathbf{k}/|\mathbf{r}|$, $J(\nu) = \int d\mu I(\mu, \nu)$ denotes the mean intensity, and $S_\nu(r)$ the emission function for newly created photons at frequency ν and radius r (in photons $\text{cm}^{-3} \text{s}^{-1} \text{sr}^{-1} \text{Hz}^{-1}$, see e.g. Loeb & Rybicki 1999). Furthermore, $\chi_\nu = \frac{h_P \nu_\alpha}{4\pi} \frac{B_{21}}{\sqrt{\pi} \Delta \nu_\alpha} (3n_1 - n_2) \phi(\nu)$ denotes the opacity at frequency ν (e.g. Rybicki & Lightman 1979), where h_P is Planck's constant, $\nu_\alpha = 2.46 \times 10^{15} \text{ Hz}$ is the Ly α frequency, $n_{1(2)}$ is the number density of hydrogen atoms in their electronic ground (first excited) state, B_{21} is the Einstein-B coefficient of the $2 \rightarrow 1$ transition, $\phi(\nu)$ is the line profile function (e.g. Rybicki & Lightman 1979, their Eq. 1.79), and $\Delta \nu_\alpha = \frac{v_{th}}{c}$. Here, v_{th} is the thermal velocity of the hydrogen atoms in the gas, given by $v_{th} = \sqrt{2k_B T/m_p}$,

where k_B is the Boltzmann constant, T the gas temperature, and m_p the proton mass.

Under the assumption that $I(\nu, \mu)$ has only a weak dependence on direction (which is reasonable given that Ly α radiation scatters very frequently), $I(\nu, \mu)$ can be expressed as a first-order Taylor expansion in μ , i.e. $I(\nu, \mu) = a(\nu) + b(\nu)\mu$. In this so-called ‘‘Eddington approximation’’, the expression for flux simplifies to (e.g. Rybicki & Lightman 1979, their Eq. 1.118)

$$H(\nu) = \frac{1}{3} \frac{dJ(\nu)}{d\tau} = \frac{c}{12\pi} \frac{du(\nu)}{d\tau}, \quad (4)$$

where we have used the relation, $u = 4\pi J/c$, in which $u(\nu)$ is the specific energy density in the radiation field at a frequency ν . Furthermore, we have decoupled the gas' absorption and emission functions from the Ly α radiation field, and assumed that all neutral hydrogen atoms are in their electronic ground state (this assumption is justified in more detail in Appendix A), i.e. $n_2 = 0$ and $n_1 = n_H$. Under this assumption, $d\tau = \chi_\nu dr = n_H \sigma(\nu) dr$ with n_H being the number density of neutral hydrogen atoms. Substituting this expression back into Eq. (2) yields

$$F_{\text{rad}} = \frac{1}{3n_H} \frac{d}{dr} \int d\nu u(\nu) = \frac{1}{3n_H} \frac{dU}{dr}, \quad (5)$$

where we defined $U \equiv \int d\nu u(\nu)$. Note that the cross-section does not appear in the final expression for the radiation force¹.

2.1 Implementation in Monte-Carlo Technique

In our Monte-Carlo simulation we sample the gas density and velocity fields with $N_s = 5000$ concentric spherical shells. The radius, thickness, and volume of shell j are denoted by r_j , dr_j , and V_j , respectively. We compute the radiation force using two approaches:

- In the first approach, we calculate the energy density (U in Eq. 5) in the Ly α radiation field as a function of radius: Using the Monte-Carlo simulation we compute the average time that photons spend in shell j , which we denote by $\langle t \rangle_j$. The total number of photons that is present in shell j at any given time is then given by $N_{\alpha,j} = \dot{N}_\alpha \times \langle t \rangle_j$, where \dot{N}_α is the rate at which photons are emitted. This yields the energy density, $U_j = N_{\alpha,j} h\nu_\alpha / V_j$. Finally, Eq. (5) is used to compute the radiation force on atoms in shell j . Note that estimators of the energy density in -and the momentum transfer by- a radiation field in a more general context is discussed by e.g. Lucy (1999) and Lucy (2007).

- In the second approach, we calculate the momentum transfer from a Ly α photon to an atom in each scattering event, $\Delta p = h_P(\mathbf{k}_{\text{in}} - \mathbf{k}_{\text{out}})/2\pi$. Here, \mathbf{k}_{in} and \mathbf{k}_{out} are the photons wavevectors before and after scattering. We compute the average *total momentum transfer* (i.e. summed over all scattering events) per photon in shell j , $\langle \Delta \mathcal{P} \rangle_j$, and obtain the total momentum transfer from $\dot{P}_{\alpha,j} = \dot{N}_\alpha \times \langle \Delta \mathcal{P} \rangle_j$. The force on an individual atom is obtained by dividing by the total number of hydrogen atoms in shell j , i.e. $F_j = \dot{P}_{\alpha,j} / (V_j \times n_{H,j})$.

¹ The right-hand-side of Eq. (5) is analogous to the usual pressure gradient force in fluid-dynamics which is not dependent on the scattering cross-section of the fluid particles.

Both methods should give identical results, provided that the Eddington approximation holds.

2.2 Test Case: Sources in a Neutral Comoving IGM

We begin by considering a Ly α point source at a redshift $z = 10$ embedded in a neutral intergalactic medium (IGM) that is expanding with the Hubble flow. The photons scatter and diffuse away from the source while Hubble expansion redshifts the photons away from resonance. In this case, the angle-averaged intensity $J(\nu)$ and its radial dependence can be calculated analytically (Loeb & Rybicki 1999). The availability of analytic expressions for $J(\nu, r)$, and therefore the radiation force F_{rad} (through Eq. 5), makes this a good test case for our code.

In Figure 1 we plot the radial dependence of the energy density (in erg cm^{-3}) in the Ly α radiation field for a model in which the central source is emitting $\dot{N}_{\alpha,54} \times 10^{54}$ photons s^{-1} (where we have introduced the dimensionless quantity $\dot{N}_{\alpha,54} \equiv (\dot{N}_{\alpha}/10^{54} \text{ photons s}^{-1})$). This corresponds to a luminosity of $L_{\alpha} = \dot{N}_{\alpha,54} \times 1.6 \times 10^{43} \text{ erg s}^{-1}$, which represents a bright Ly α emitting galaxy (e.g. Ouchi et al. 2008). The *blue dotted line* shows the energy density if the IGM were fully transparent to Ly α radiation. In this hypothetical case all photons stream radially outward, and the energy density is given by $L_{\alpha}/(4\pi r^2 c)$. The *red dashed line* shows the energy density, $U(r) = \frac{4\pi}{c} \int d\nu J(\nu, r)$, derived from the analytic expression for $J(r, \nu)$ given in Loeb & Rybicki (1999, their Eq. 21), while the *black histogram* shows the energy density extracted from the simulation (§ 2.1). Clearly, the analytic and Monte-Carlo calculations yield consistent results. Scattering reduces the effective speed at which photons propagate radially outward, which enhances their energy density (especially at small radii) relative to the transparent case. At sufficiently large distances however, the photons have redshifted far enough from resonance that they are propagating almost freely to the observer, and the energy density approaches $L_{\alpha}/4\pi r^2 c$. We note that at a sufficiently high value of $\dot{N}_{\alpha,54}$, the fraction of hydrogen atoms that populate the 2p (and 2s) levels is non-negligible and our assumption that (almost) all of the atoms populate their electronic ground state becomes invalid (so that the solution for $U(r)$ in Figure 1 breaks down). However, as we show in Appendix A, this only occurs when $\dot{N}_{\alpha,54} \gtrsim 10^7$, well beyond the regime considered in this paper.

In Figure 2 we compare the radiation force to the gravitational force on a single hydrogen atom, $F_{\text{grav}} = GM(< r)m_p/r^2$, where $M(< r)$ is the total mass enclosed within a radius r . We plot the ratio $F_{\text{rad}}/F_{\text{grav}}$ scaled by $M = 10^{11} M_{\odot}$. The *black dotted line* (*grey solid histogram*) was calculated by applying Eq. (5) to the energy density $U(r)$ that was obtained by using the analytic (Monte-Carlo) approach (also see Fig 1). For comparison, the *black solid histogram* was obtained by directly computing the momentum transfer rate from photons to atoms as outlined in § 2.1.

² The number density of halos more massive than $10^{11} M_{\odot}$ at $z = 10$ is $\sim 10^{-7} \text{ comoving Mpc}^{-3}$, implying that these rare halos are among the most massive ones in existence at that early cosmic time.

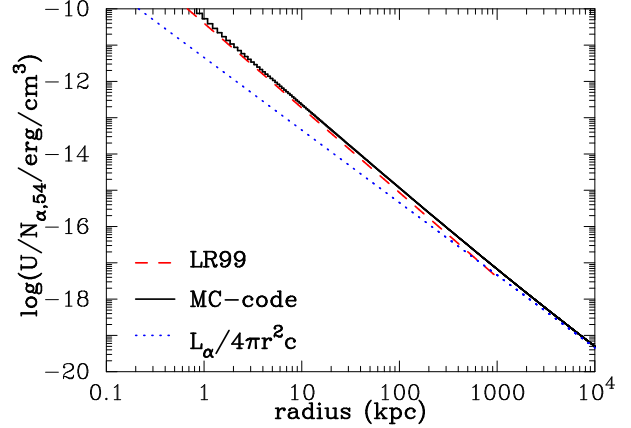


Figure 1. Radial profile of the energy density $U(r)$ (erg cm^{-3}) in the Ly α radiation field surrounding a central source that is emitting $\dot{N}_{\alpha,54} \times 10^{54}$ photons s^{-1} into an expanding neutral IGM. The *blue dotted line* shows $U(r)$ if the IGM were fully transparent. The *black solid* (*red dashed*) line shows $U(r)$ when radiative transfer is included using an analytic (Monte-Carlo) approach (see text). Scattering reduces the speed at which Ly α photons are propagating radially outward, increasing $U(r)$ relative to the transparent case.

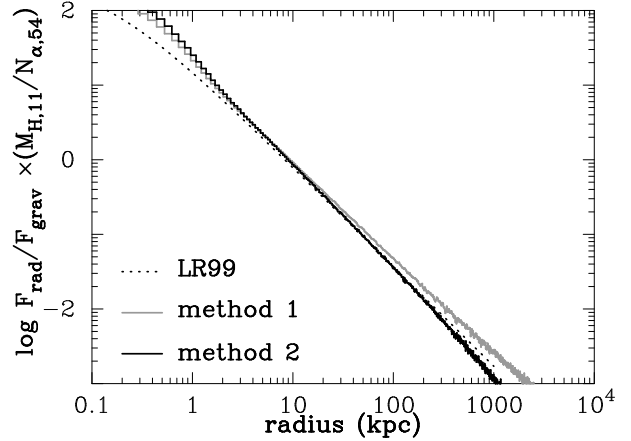


Figure 2. The ratio of radiation to gravitational force on a hydrogen atom as a function of physical radius in kpc. To scale out the dependence of this ratio on halo mass, M_h , and production rate of Ly α photons by the central source, \dot{N}_{α} , the vertical axis is normalized by $M_{h,11}/\dot{N}_{\alpha,54}$ (see text). The *black dotted* (*grey solid*) line was obtained by applying Eq. (5) to the energy density $U(r)$ that was obtained by using the analytic (Monte-Carlo) approach (see Fig 1). The *black solid line* was obtained by directly computing the momentum transfer rate from photons to atoms in the Monte-Carlo code as outlined in § 2.1. The results demonstrate that (i) the radiation force exceeds gravity at $r < 10(\dot{N}_{\alpha,54}/M_{h,11})$ kpc, and (ii) both methods yield consistent results.

Figure 2 shows that the radiation force overwhelms gravity at small radii. The energy density scales approximately as $\partial \log U / \partial \log r \sim -2.3$ (Fig 1). Therefore, $F_{\text{rad}}/F_{\text{grav}} \propto r^{-1.3}$ and reaches unity at $r \sim 10$ physical kpc.

The radiation force increases linearly with \dot{N}_{α} while the gravitational force scales as M . Thus, $F_{\text{rad}}/F_{\text{grav}}$ scales linearly with the ratio $\mathcal{R} \equiv \dot{N}_{\alpha}/M$. To scale out the dependence on \mathcal{R} , the vertical axis shows the quantity

$(F_{\text{rad}}/F_{\text{grav}}) \times (M_{11}/\dot{N}_{\alpha,54})$, where $M_{11} = (M/10^{11} M_{\odot})$. For example, if $M_{11} = 0.1$ then Figure 2 shows that radiation pressure exceeds gravity out to $r = 100$ kpc, well beyond the virial radius of a halo of this mass at $r_{\text{vir}} \sim 6.6$ kpc.

Most importantly, Figure 2 shows that the two approaches used to compute the radiation force in the simulation yield consistent results, with a noticeable deviation only at the largest radii ($r \sim 1$ Mpc). At large radii most photons stream outwards radially and the Eddington approximation that was used to derive Eq. (4) becomes increasingly unreliable.

Next, we use the radiative transfer code to explore the magnitude of the Ly α radiation pressure for a range of models which represent an evolutionary sequence of structure formation in the Universe. We focus on the Ly α radiation pressure on gas surrounding (i) the first stars (§ 3.1); (ii) the first galaxies (§ 3.2); and (iii) the interstellar medium of galaxies (§ 3.3).

3 RESULTS

3.1 Case I: A Single Massive Star in a Minihalo

Numerical simulations of structure formation suggest the first stars that formed in our Universe were massive ($M_{*} \sim 100 M_{\odot}$), and formed as single objects in dark matter halos with masses of $M \sim 10^6 M_{\odot}$ that collapsed at $z > 10$ (e.g. Haiman et al. 1996; Abel et al. 2002; Yoshida et al. 2006). Here, we focus our attention on a star with a mass $M_{*} = 100 M_{\odot}$ that formed at $z = 15$ in a dark matter mini-halo of mass $M = 2 \times 10^6 M_{\odot}$. The star emits 10^{50} ionizing photons per second (Schaerer 2002; Abel et al. 2007). We assume that the ionizing flux ionizes all the gas out to the virial radius of the dark matter halo ($r_{\text{vir}} = 0.26$ kpc) but not beyond that radius (Kitayama et al. 2004). Hence, the IGM gas surrounding this central source is assumed to be neutral ($x_{\text{HI}} = 1.0$) and cold ($T_{\text{gas}} = 300\text{K}$, which corresponds to the temperature of the neutral IGM at $z = 15$ due to X-Ray heating, see e.g. Fig 1 of Pritchard & Loeb 2008).

Recombination following photoionization converts $\sim 68\%$ of all ionizing photons into Ly α photons (Osterbrock 1989, p 387). Hence, the entire halo is a Ly α source that is surrounded by neutral intergalactic gas. To determine the radial dependence of the Ly α production rate (S_{ν} in Eq. 3), we need to specify the gas density profile. We assume that the gas distribution inside the dark matter halo is described by an NFW-profile with a concentration parameter $C = 5$ and a thermal core³ at $r < 3r_{\text{vir}}/4C$ (see Maller & Bullock 2004). We point out however, that our final results are not sensitive to our choice of $S_{\nu}(r)$.

Once $S_{\nu}(r)$ has been determined, we find the radius, r , at which a Ly α photon is generated in the Monte-Carlo simulation from the relation

$$R = \frac{1}{N} \int_0^r dr 4\pi r^2 n_{\text{H}}^2 \alpha_{\text{rec}}, \quad (6)$$

³ With this gas density profile, the total recombination rate inside the dark matter halo is $\int_0^{r_{\text{vir}}} dr 4\pi r^2 n_{\text{H}}^2 \alpha_{\text{rec}} \sim 4.5 \times 10^{49} \text{ s}^{-1}$. The total recombination rate can be increased to balance the photoionization rate by introducing a clumping factor $K \equiv \langle n_{\text{H}}^2 \rangle / \langle n_{\text{H}} \rangle^2 \sim 2$.

where R is a random number between 0 and 1, $N = \int_0^{r_{\text{vir}}} dr 4\pi r^2 n_{\text{H}}^2 \alpha_{\text{rec}}$ is the total recombination rate inside the dark matter halo, and $\alpha_{\text{rec}} = 2.6 \times 10^{-13} \text{ cm}^3 \text{ s}^{-1}$ is the case-B recombination coefficient at a temperature $T = 10^4$ K (e.g. Hui & Gnedin 1997). Once the photon is generated, it scatters through the neutral IGM until it has redshifted far enough from resonance that it can escape to the observer.

In the *left panel* of Figure 3 we show the energy density (in erg cm^{-3}) of the Ly α radiation field as a function of radius. The *red solid* line represents a model in which we assumed the IGM to follow the mean density and Hubble expansion right outside the virial radius. The *blue dotted* line shows a more realistic model in which the IGM is still overdense near the virial radius, and in which the intergalactic gas is gravitationally pulled towards the minihalo (see Dijkstra et al 2007 for a quantitative description of the density and velocity profiles based on the model of Barkana 2004). The *black dashed* line shows the same model as the *red solid* line but with the neutral fraction increasing linearly between r_{vir} and $2r_{\text{vir}}$. This provides a better representation of the fact that the central population III star emits ionizing photons with energies $\gtrsim 54$ eV, which can photoionize hydrogen (and helium) atoms that lie deeper in the IGM. The goal of this model is to investigate whether our results depend sensitively on the presence of a sharp boundary between HI and HII.

All models show that the radiation energy density within the fully ionized minihalo ($r \lesssim r_{\text{vir}} = 0.26$ kpc) has only a weak dependence on radius, i.e. $d \log U / d \log r \gtrsim -1$. Naively, this may appear surprising given the fact that within the model, no scattering occurs within the virial radius and one may expect the energy density in the Ly α radiation field to scale as $U \propto r^{-2}$. However, in reality U obtains only a weak radial dependence because the radiation can be scattered back into the ionized minihalo as soon as it 'hits' the wall of neutral IGM gas. Ly α photons are therefore trapped inside the ionized minihalo and their energy density is boosted to a value that is only weakly dependent on radius. On the other hand, for $r \gtrsim r_{\text{vir}}$ we find that $d \log U / d \log r \lesssim -2$, which is because Ly α photons are trapped more efficiently near the edge of the HII region, while they stream freely outwards at larger radii (as in § 2.2 and Fig 1). Figure 3 shows clearly that the radial dependence of the Ly α energy density is not sensitive to the detailed model assumptions about the gas in the IGM.

In the *right panel* of Figure 3 we show the ratio between the radiation force (Eq. 5) and the gravitational force on a single hydrogen atom), $F_{\text{grav}} = GM(< r)m_{\text{p}}/r^2$, where $M(< r)$ is the total (baryons + dark matter) mass enclosed within a radius r . In all models, radiation pressure dominates over gravity by as much as $\gtrsim 2$ orders of magnitude. The radiation force is largest for the models in which the IGM is assumed to be at mean density, because of the n_{H}^{-1} factor in the equation for the radiation force (Eq. 5). Note that the spike near $r \sim 2.6$ kpc for the other two models is due to an artificial discontinuity in the IGM velocity field that exists in this model.

Ly α radiation pressure may operate throughout the lifetime of the central star. Over a lifetime of ~ 2.5 Myr (see Table 4 of Schaerer 2002), this mechanism is capable of accelerating the gas to velocities of 10 (50) km s^{-1} at $r = 0.3$ kpc in the model represented by the *blue dotted* (*red solid*)

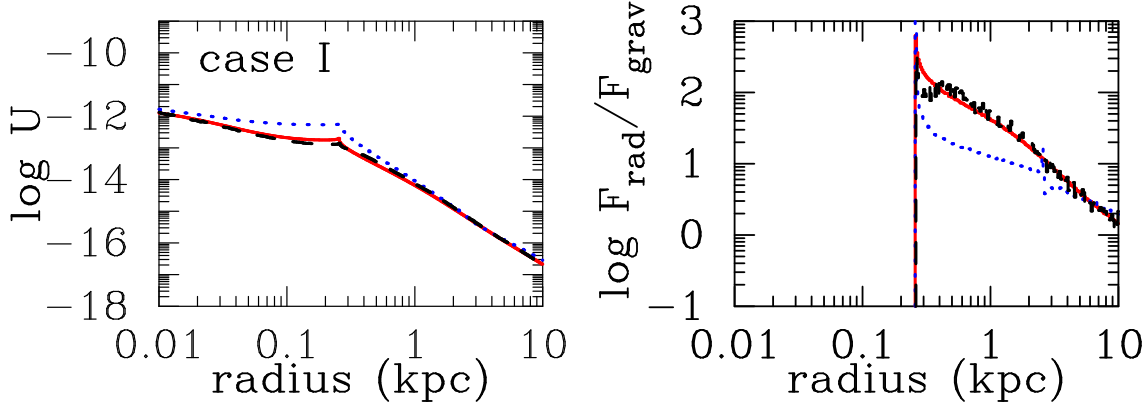


Figure 3. The energy density in the Ly α radiation field (*left panel*), and the ratio between the radiation and the gravitational forces (*right panel*) for a single very massive star ($M_* = 100M_\odot$) in a minihalo $M_h = 2 \times 10^6 M_\odot$. The *red solid line* represents a model in which the IGM is at the mean cosmic density and undergoes Hubble expansion right outside the virial radius at $r = 0.26$ kpc. The *blue dotted line* shows a more realistic model in which the IGM is overdense near the virial radius, and in which the intergalactic gas is gravitationally pulled towards the minihalo (see text). The *black dashed line* shows the same model as the *red solid line* but with the neutral fraction increasing linearly between r_{vir} and $2r_{\text{vir}}$. The star ionizes all the gas out to the virial radius. Ly α photons freely propagate until they reach the edge of the HII region, where they are likely to be scattered back into the ionized minihalo. This yields an almost constant radiation energy density. Once outside the HII region, the radiation force dominates over gravity out to $r = 10$ kpc and may accelerate neutral gas outside the HII region to velocities of order $\sim 10 \text{ km s}^{-1}$.

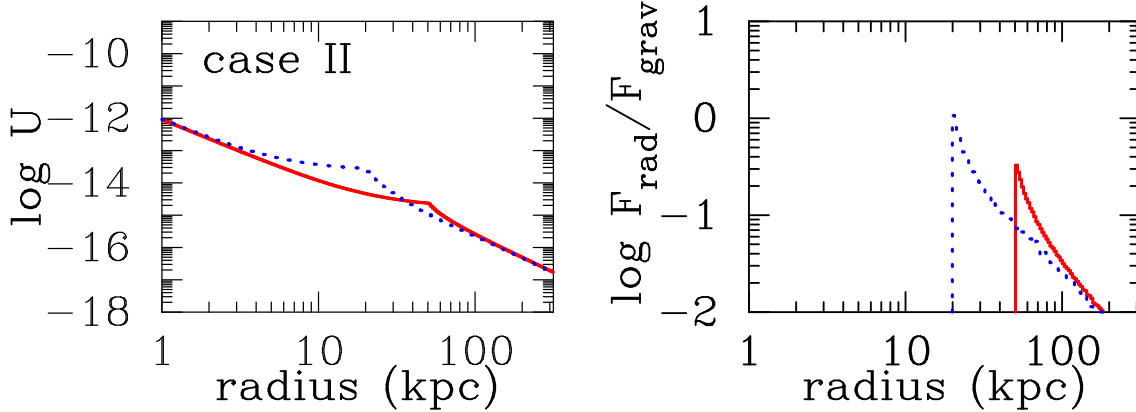


Figure 4. Same as Figure 3, but for the case of a star forming galaxy ($\dot{M}_* = 0.34M_\odot \text{ yr}^{-1}$, see text), surrounded by an HII region with a radius $R_{\text{HII}} = 50$ kpc ($R_{\text{HII}} = 20$ kpc) for the *solid line* (*dotted line*), which is in turn surrounded by a fully neutral intergalactic medium (IGM). For the assumed total halo mass of $M_{\text{tot}} = 10^9 M_\odot$, the pressure exerted by the Ly α photons is not large enough to exceed gravity. However, radiation pressure wins for $M_{\text{tot}} = 10^8 M_\odot$, but even in this case the radiation force is not large enough to produce a significant wind speed in the IGM (see text).

line, and to 4 (16) km s^{-1} at $r = 0.4$ kpc (the reason for this large difference is that the edge of the HII region lies at $r = 0.26$ kpc. Hence, gas at $r = 0.3$ kpc is separated by 0.04 kpc from this edge, while gas at $r = 0.4$ kpc is separated by a distance that is 3.5 times larger).

Thus, Ly α radiation pressure can accelerate the gas to velocities that exceed the escape velocity from the dark matter halo ($v_{\text{esc}} \sim \sqrt{2}v_{\text{circ}} \sim 8 \text{ km s}^{-1}$) as well as the sound speed of the intergalactic medium ($c_s = 2.2(T_{\text{gas}}/300 \text{ K})^{1/2} \text{ km s}^{-1}$).

Note that as the gas is pushed out and its velocity profile changes, the subsequent radiative transfer is altered. For example, we repeated the radiative transfer calculation for models in which gas at $r_{\text{vir}} < r \lesssim 2r_{\text{vir}}$ was accelerated to velocities in the range $10 - 20 \text{ km s}^{-1}$ (outward) and found a slightly shallower profile for $U(r)$ which lowered the radi-

ation force by a factor of ~ 3 . Consequently, the acceleration of the gas decreases with time and the actual velocities reached by the gas are lower than the estimates given above by a factor of a few. Nevertheless, the resulting velocities are still substantial.

Our calculations imply that Ly α radiation pressure can affect the gas dynamics in the IGM surrounding minihalos that contain the first stars. The impact of Ly α radiation pressure increases with decreasing density of the surrounding gas in the IGM. In practice, the distribution of the IGM is not spherically symmetric. Instead, the density is expected to vary from sightline to sightline (being large along filaments and small along voids). Our results imply that Ly α radiation pressure will be most efficient in 'blowing out' the lower density gas. This conjecture is supported by the tendency of Ly α photons to preferentially scatter through the low-density gas; their propagation along the path of least re-

sistance would naturally boost up the Ly α flux there. This effect will be moderated by the tendency of the HII region around the first stars to extend further into the low density gas (in ‘butterfly’-like patterns, e.g. Abel et al, 1999).

If the central star dies in a supernova explosion, then the resulting violent outflow could blow most of the baryons out from the minihalo. However, stars with masses in the range $30M_{\odot} \lesssim M_{*} \lesssim 140M_{\odot}$ and $M_{*} \gtrsim 260M_{\odot}$, are not expected to end their lives in a supernova. Instead, these stars collapse directly to a black hole (Heger & Woosley 2002) and have weak winds (because of the lack of heavy elements in their atmosphere), so that radiation pressure may be the dominant process that affects their surrounding IGM.

In summary, Ly α radiation pressure on the neutral IGM around minihalos in which the first stars form, can exceed gravity by orders of magnitude and launch supersonic winds. Our limited analysis does not allow a detailed discussion on the consequences of these winds. This requires 3D simulations with cosmological initial conditions that capture the full IGM density field around the minihalo and that track the evolution of the shocks that may form in the IGM. Such simulation are numerically challenging as they require self-consistent treatment of gas dynamics and Ly α radiative transfer in a moving inhomogeneous medium.

3.2 Case II: A Young Star Forming Galaxy

Our second case concerns a young galaxy that is forming multiple stars in a dark matter halo of mass $M = 10^9 M_{\odot}$ at $z = 10$. We assume that the galaxy is converting a fraction $f_{*} = 10\%$ of its baryons into stars over $\sim 0.1t_{\text{H}}$ (Wyithe & Loeb 2006), where $t_{\text{H}} = [2/3H(z)] \sim 0.49$ Gyr, is the age of the Universe at $z = 10$. This translates to a star formation rate of $\dot{M}_{*} = 0.34M_{\odot} \text{ yr}^{-1}$. For population III stars forming out of pristine gas, the total emission rate of ionizing photons is $\dot{N}_{\text{ion}} \sim 3 \times 10^{53} \text{ s}^{-1}$ (Schaerer 2002)⁴. If $\sim 1\%$ of the ionizing photons escape from the galaxy (Chen et al. 2007; Gnedin et al. 2008), then this translates to a Ly α luminosity of $L_{\alpha} = 3 \times 10^{42} \text{ erg s}^{-1}$. Furthermore, this galaxy can photoionize a spherical HII region of a radius $R_{\text{HII}} \sim 50$ physical kpc. Note however, that other ionizing sources would likely exist within this HII region. Indeed, clusters of sources are thought to determine the growth of ionized bubbles during reionization. This results in a characteristic HII region size that is significantly larger than that produced by single source, especially during the later stages of reionization (e.g. Furlanetto et al. 2004; McQuinn et al. 2007). In this framework, our model represents a star forming galaxy during the early stages of reionization or alternatively a galaxy that lies 50 kpc away from the edge of a larger ionized bubble.

In this particular case, the majority of all recombination events occur in the central galaxy. Thus, we initiate all Ly α photons at $r = 0$ in the Monte-Carlo simulation. We assume that the gas is completely ionized out to $R_{\text{HII}} = 50$ kpc, beyond which it is neutral. As shown in § 3.1, this abrupt

transition in the ionized fraction of H in the gas does not affect our results.

The *left panel* of Figure 4 shows the energy density (in erg cm^{-3}) of the Ly α radiation field as a function of radius. The *solid line* represents the model discussed above. A kink in the energy density is seen at the edge of the HII region (see § 3.1 for a more detailed discussion of the profile). The *dotted line* represents a variant of the model in which we have reduced the size of the HII region to $R_{\text{HII}} = 20$ kpc.

The *right panel* of Figure 4 shows the ratio between the radiation and the gravitational forces on a single hydrogen atom. In our fiducial model, the radiation force does not exceed gravity; rather, at the edge of the HII region, gravity is ~ 3 times stronger. The radiation force becomes equal to the gravitational force if $R_{\text{HII}} = 20$ kpc. This requires an extremely low [by a factor $\sim (50/20)^3$] escape fraction of ionizing photons, $f_{\text{esc}} \sim 6 \times 10^{-4}$.

Alternatively, radiation pressure *is* important when the halo mass of the star forming region is reduced to $10^8 M_{\odot}$. Halos of this mass are the the most abundant halos at $z \sim 10$ that are capable of cooling via excitation of atomic hydrogen (i.e. their virial temperature just exceeds $T_{\text{vir}} \sim 10^4$ K, e.g. Barkana & Loeb 2001). The total gas reservoir inside these halos is $M_{\text{b}} = \frac{\Omega_{\text{b}}}{\Omega_{\text{m}}} M_{\text{tot}} \sim 1.5 \times 10^7 M_{\odot}$, and so these halos can sustain a star formation rate of $\dot{M}_{*} = 0.3M_{\odot} \text{ yr}^{-1}$ for up to ~ 50 Myr. However, even if the radiation force is allowed to operate for ~ 50 Myr, we find that radiation pressure cannot accelerate the gas in the IGM to velocities that exceed $\sim 1 \text{ km s}^{-1}$. We therefore conclude that although Ly α pressure may exceed gravity in the neutral IGM that surrounds HII regions around $M_{\text{tot}} = 10^8 M_{\odot}$ halos, the absolute magnitude of the radiation force is too weak to drive the IGM to supersonic velocities.

3.3 Case III: Ly α Driven Galactic Supershells

In principle, Ly α radiation pressure can be important when neutral gas exists in close proximity to a luminous Ly α source. So far, we focused our attention on HI gas in the IGM. However, neutral gas in the interstellar medium (ISM) of the host galaxy is located closer to the Ly α sources and should be exposed to an even stronger Ly α radiation pressure. Indeed, it has been demonstrated (e.g. Ahn & Lee 2002; Verhamme et al. 2008) that scattering of Ly α photons by neutral hydrogen atoms in a thin (with a thickness much smaller than its radius), outflowing ‘supershell’ of HI gas surrounding the star forming regions can naturally explain two observed phenomena: (i) the common shift of the Ly α emission line towards the red relative to metal absorption lines and the host galaxy’s systemic redshift determined from other nebular recombination lines (e.g. Pettini et al. 2001; Shapley et al. 2003); and (ii) the asymmetry of the Ly α line with emission extending well into its red wing (e.g. Lequeux et al. 1995; Tapken et al. 2007).

The existence of thin, outflowing shells of neutral atomic hydrogen around HII regions is confirmed by HI-observations of our own Milky-Way (Heiles 1984) and other nearby galaxies (e.g. Ryder et al. 1995). The largest of these shells, so-called ‘supershells’, have radii of $r_{\text{max}} \sim 1$ kpc (e.g. Ryder et al. 1995; McClure-Griffiths et al. 2002) and HI column densities in the range $N_{\text{HI}} \sim 10^{19} -$

⁴ More precisely, the ionizing photon production rate is $\sim 10^{54} \text{ s}^{-1} \times (\text{SFR}/M_{\odot} \text{ yr}^{-1})$ in the no-mass-loss model of Schaerer (2002) in which metal-free stars form according to a Salpeter IMF with $M_{\text{low}} = 1M_{\odot}$ and $M_{\text{high}} = 500M_{\odot}$ (his model ‘B’).

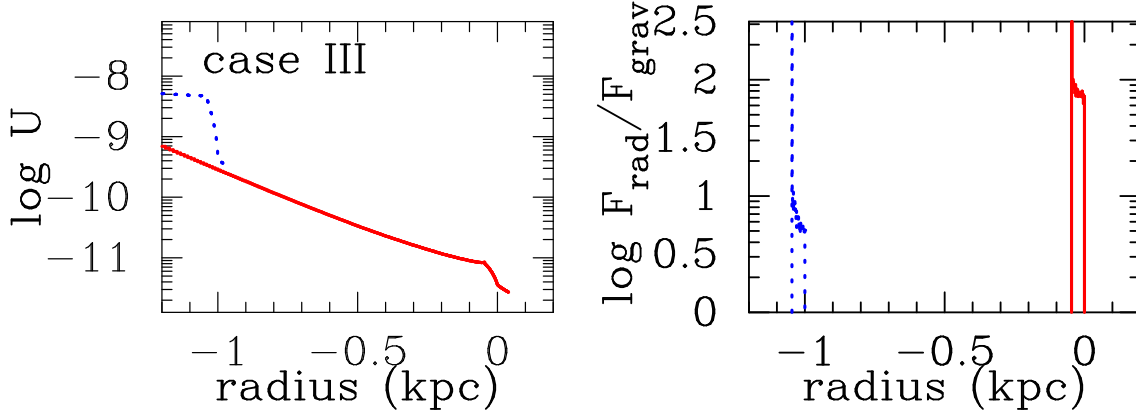


Figure 5. Same as in Figure 3 and Figure 4, but for models in which a central Ly α source of luminosity L_α is surrounded by a thin ($r_{\text{sh,min}} = 0.9r_{\text{sh,max}}$) spherical shell of HI that is expanding at $v_{\text{sh}} = 200 \text{ km s}^{-1}$. The blue dotted lines (red solid lines) represent a model in which $N_{\text{HI}} = 10^{21} \text{ cm}^{-2}$ and $r_{\text{sh,max}} = 0.1 \text{ kpc}$ ($N_{\text{HI}} = 10^{19} \text{ cm}^{-2}$ and $r_{\text{sh,max}} = 1.0 \text{ kpc}$). When calculating F_{grav} , we assumed the total mass enclosed by the supershell to be $10^8 M_\odot$ (see text). The results strongly suggest that Ly α radiation pressure may be dynamically important in the interstellar medium of galaxies. The total radiation force on the shell (obtained as a sum over all atoms) may be computed via $F_{\text{tot}} = M_F L_\alpha / c$, where M_F may be thought of as a force multiplication factor that depends both on the shell's outflow speed, v_{exp} , and its HI column density, N_{HI} . The dependence of M_F on these parameters is shown in Fig 6.

10^{21} cm^{-2} (e.g. Lequeux et al. 1995; Kunth et al. 1998; Verhamme et al. 2008). Supershells are thought to be generated by stellar winds or supernovae explosions which sweep-up gas into a thin expanding neutral shell (see e.g. Tenorio-Tagle & Bodenheimer 1988, for a review). The back-scattering mechanism attributes both the redshift and asymmetry of the Ly α line to the Doppler boost that Ly α photons undergo as they scatter off the outflow on the far side of the galaxy back towards the observer (e.g. Lee & Ahn 1998; Ahn & Lee 2002; Ahn et al. 2003; Ahn 2004; Verhamme et al. 2006, 2008). It is interesting to investigate whether Ly α radiation pressure may provide an alternative mechanism that determines the supershell kinematics.

In Figure 5 we show the energy density (*left panel*) and the Ly α radiation force (*right panel*) for two models. Both models assume that: (i) there is a Ly α source at $r = 0$ with a luminosity of $L_\alpha = 10^{43} \text{ erg s}^{-1}$; (ii) the emitted Ly α spectrum prior to scattering has a Gaussian shape as a function of photon frequency with a Doppler velocity width of $\sigma = 50 \text{ km s}^{-1}$; (iii) the spatial width of the supershell is 10% of its radius; and (iv) the shell has an outflow velocity of $v = 200 \text{ km s}^{-1}$. The blue dotted (red solid) lines represent a model in which the supershell has a column density of $N_{\text{HI}} = 10^{21}$ ($N_{\text{HI}} = 10^{19}$) cm^{-2} and a maximum radius that is $r_{\text{sh}} = 0.1 \text{ kpc}$ ($r_{\text{sh}} = 1.0 \text{ kpc}$). Our calculations assume that there is no neutral gas (or dust) interior to the HI supershell.

The *left panel* of Figure 5 shows that inside the supershell the energy density decreases more gradually than r^{-2} because of photon trapping (similarly to the previously discussed cases in § 3.1-§ 3.2). The shell with the larger column of HI is more efficient at trapping the Ly α photons, and thus yields a flatter energy density profile. In both models the energy density drops steeply within the supershell (the energy density decreases as r^{-2} outside the shell, if no scattering occurs here).

The *right panel* of Figure 5 shows the ratio between the radiation and gravitational forces. Towards the center

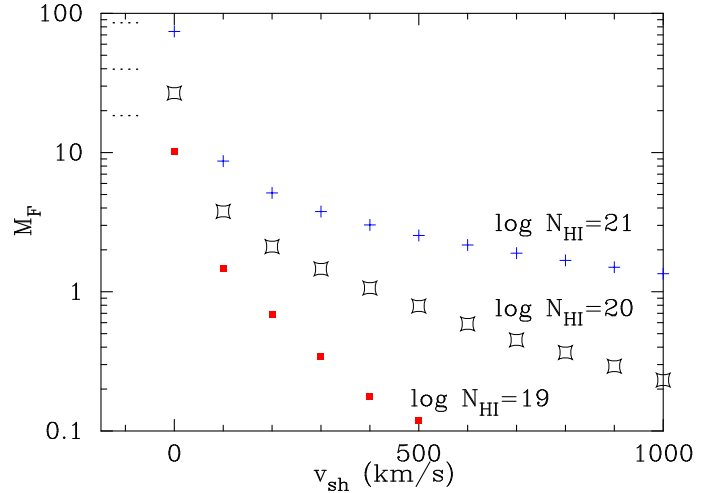


Figure 6. The multiplication factor M_F provides the total force that Ly α photons exert on a spherical HI shell, $F_{\text{tot}} = M_F L_\alpha / c$, where L_α is the Ly α luminosity of the source in erg s^{-1} and c is the speed of light. The plot shows M_F as a function of the expansion velocity of the HI shell, v_{sh} , for three values of HI column density, and under the assumption that the HI shell surrounds an empty cavity. The parameter M_F provides a measure of the efficiency by which Ly α photons can be ‘trapped’ by the shell of HI gas. Thus, M_F increases with increasing N_{HI} and decreasing v_{sh} . The dotted horizontal lines show the values of M_F that have been derived in the past (for a static, uniform, infinite slab of material e.g. Adams 1975).

of the dark matter halo, baryons dominate the mass density and an evaluation of F_{grav} requires assumptions about the radial distribution of the baryons. For simplicity, we consider a fixed total mass interior to the supershell of $M(< r) = 10^8 M_\odot$, so that $F_{\text{grav}}(r) = GM(< r)m_p/r^2$. Note that any assumed mass profile $M(< r)$ will not affect the results as long as $F_{\text{rad}} \gg F_{\text{grav}}$.

We find that the radiation force exceeds gravity in both examples under consideration. For $N_{\text{HI}} = 10^{21} \text{ cm}^{-2}$

and $r_{\text{sh}} = 0.1$ kpc, $F_{\text{rad}} \sim 10F_{\text{grav}}$. Thus, radiation pressure would have been important even if we had chosen $M \sim 10^9 M_{\odot}$. In the model with $N_{\text{HI}} = 10^{19} \text{ cm}^{-2}$ and $r_{\text{sh}} = 1.0$ kpc, $F_{\text{rad}} \sim 10^2 F_{\text{grav}}$, and radiation pressure would have been important even if $M \sim 10^{10} M_{\odot}$. Hence, our calculations strongly suggest that $\text{Ly}\alpha$ radiation pressure may be dynamically important in the ISM of galaxies.

The total $\text{Ly}\alpha$ radiation force is obtained by summing the force over all atoms in the supershell. It is interesting to compare this force to L_{α}/c . The latter quantity denotes the total momentum transfer rate (force) from the $\text{Ly}\alpha$ radiation field to the supershell under the assumption that each $\text{Ly}\alpha$ photon is re-emitted isotropically after entering the shell (including multiple scatterings inside the supershell). In Figure 6 we plot the quantity M_F which is defined as

$$M_F \equiv \frac{\sum_{\text{atoms}} F_{\text{rad}}}{L_{\alpha}/c}, \quad (7)$$

as a function of the expansion velocity of the shell, v_{sh} for three different values of N_{HI} .

Figure 6 shows that M_F , which can be thought of as a force multiplication factor⁵, greatly exceeds unity for low shell velocities and large HI column densities. The parameter M_F is related to the mean number of times that a $\text{Ly}\alpha$ photon ‘bounces’ back and forth between opposite sides of the expanding shell. For example, $M_F = 1$ when all $\text{Ly}\alpha$ photons enter the shell, scatter once, and then escape from the shell in no preferred direction. On the other hand, $M_F = 3$ when all $\text{Ly}\alpha$ photons enter the shell, scatter back towards the opposite direction, and then escape in no preferred direction after scattering in the shell for a second time. A schematic illustration of this argument is provided in Figure 7. Note that when $M_F = 1$ ($M_F = 3$), each photon spends on average a timescale of r_{sh}/c ($3r_{\text{sh}}/c$) in the bubble enclosed by the shell. In other words, the factor M_F relates to the ‘trapping time’, t_{trap} , that denotes the total time over which $\text{Ly}\alpha$ photons are trapped inside the supershell⁶ (see § 1) through the relation $M_F = t_{\text{trap}}/(r_{\text{sh}}/c)$. Indeed, when $v_{\text{sh}} \rightarrow 0$ we find that M_F reproduces the value $15(\tau_0/10^{5.5})$ (indicated by *horizontal dotted lines*) that was found by Adams (1975) and Bonilha et al. (1979) reasonably well (keeping in mind

⁵ This term derives from the (time-dependent) force-multiplication function $M(t)$ that was introduced by Castor et al. (1975), as $F_{\text{rad}} \equiv M(t)(\tau_e L_{\text{bol}}/c)$. Here, F_{rad} is the total force that radiation exerts on a medium, τ_e is the total optical depth to electron scattering through this medium. The function $M(t)$ arises because of the contribution of numerous metal absorption lines to the medium’s opacity, and can be as large as $M_{\text{max}}(t) \sim 10^3$ in the atmospheres of O-stars (Castor et al. 1975).

⁶ This argument ignores the time spent on scattering inside the supershell itself. Photons penetrate on average an optical depth $\tau = 1$ into the shell. If this corresponds to a physical distance that is significantly smaller than the thickness of the shell (denoted by Δr_{sh}), then only a tiny fraction of the photons will diffuse through the shell. Hence, when averaged over these photons, ignoring the time spent inside the supershell itself is justified. Alternatively, photons with a mean free path that is at least comparable to the thickness of the shell, only spend a time $\sim \Delta r_{\text{sh}}/c \ll r_{\text{sh}}/c$ inside the supershell, which provides a negligible contribution to the trapping time.

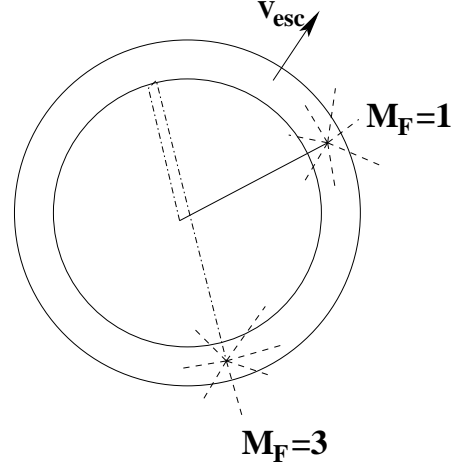


Figure 7. A schematic illustration of the origin of the force multiplication factor M_F in an expanding supershell. The $\text{Ly}\alpha$ source is located at the center of the expanding HI supershell. The *solid line* represents the trajectories of photons that enter the shell, scatter once, and then escape from the shell isotropically (indicated by the *dashed lines*). This corresponds to $M_F = 1$. On the other hand, the *dot-dashed line* represents the trajectories of photons that enter the shell, are scattered back in the opposite direction, and escape with no preferred direction after scattering in the shell for a second time. This corresponds to a case with $M_F = 3$. In general, $M_F = t_{\text{trap}}/(r_{\text{sh}}/c)$.

that these authors derived their result for a static, uniform, infinite slab of material, and assumed different frequency distributions for the emitted $\text{Ly}\alpha$ photons).

4 CONCLUSIONS

We have applied an existing Monte-Carlo $\text{Ly}\alpha$ radiative transfer code (described and tested extensively in Dijkstra et al. 2006) to the calculation of the pressure that is exerted by $\text{Ly}\alpha$ photons on an optically thick medium. This code enabled us to perform (the first) direct, accurate calculations of $\text{Ly}\alpha$ radiation pressure, which distinguishes this work from previous discussions on the importance of $\text{Ly}\alpha$ radiation pressure in various astrophysical environments.

We have focused on a range of models which represent galaxies at different cosmological epochs. In § 3.1 we have shown that the $\text{Ly}\alpha$ radiation pressure exerted on the neutral intergalactic medium (IGM) surrounding minihalos ($M_{\text{tot}} \sim 10^6 M_{\odot}$) in which the first stars form, can exceed gravity by 2–3 orders of magnitude (Fig 3), and in principle accelerate the gas in the IGM to tens of km s^{-1} . Thus, $\text{Ly}\alpha$ radiation pressure can launch supersonic winds in the IGM surrounding the first stars. Our analysis did not allow a detailed study of the consequences of these winds. A comprehensive study would require numerical simulations that capture the full IGM density field around minihalos in 3D and track the evolution of the shocks that may form in the IGM together with the $\text{Ly}\alpha$ radiative transfer. In this paper, we have also shown that $\text{Ly}\alpha$ radiation pressure is important in the neutral IGM that surrounds the HII regions produced by galaxies with a total halo mass of $M_{\text{tot}} = 10^8 M_{\odot}$ (Fig 4). These are the lowest mass, and hence the most abundant, halos in which gas can cool via atomic line excitation. Here,

however, the absolute magnitude of the radiation force is too weak to drive the gas to supersonic velocities.

Finally, we have shown in § 3.3 that the Ly α radiation pressure exerted on neutral gas in the interstellar medium (ISM) of a galaxy can also have strong dynamical consequences. In particular, we have found that the Ly α radiation force exerted on an expanding HI supershell can exceed gravity by orders of magnitude (Fig 5), for reasonable assumptions about the gravitational force. It is therefore possible that Ly α radiation pressure plays an important role in determining the kinematics of HI supershells around starburst galaxies. We have demonstrated that the total Ly α radiation force on a spherical HI supershell can be written as $F_{\text{rad}} = M_F L_\alpha / c$, where the ‘force-multiplication factor’ M_F relates to the average trapping time of Ly α photons in the neutral medium. The factor M_F can greatly exceed unity, as illustrated by Fig 6. For comparison, the maximum possible radiation force due to continuum radiation⁷ is L_{bol}/c , in which L_{bol} is the bolometric luminosity of the central galaxy. For a typical star forming galaxy, $L_\alpha \sim 0.07 L_{\text{bol}}$ (e.g. Partridge & Peebles 1967), whereas for a galaxy that contains population III stars, $L_\alpha \sim 0.24 L_{\text{bol}}$ (Schaerer 2003). Hence, the Ly α radiation pressure can dominate the maximum possible continuum radiation pressure if $M_F \gtrsim 14$ (for a normal stellar population), a threshold which is easily exceeded at large column densities of relatively slow-moving HI shells (see Fig 6).

The possibility that Ly α radiation alone can result in a radiation force that exceeds L_{bol}/c is important. Murray et al. (2005) have shown that the total momentum carried by radiation from a star-forming region can exceed the total momentum deposited by supernova explosions in it, and so galactic outflows may be driven predominantly by continuum radiation pressure. We have argued that Ly α radiation pressure may in some cases be even more important than continuum radiation pressure, and thus provide the dominant source of pressure on neutral hydrogen in the ISM.

The important implication of our last result is that Ly α radiation pressure may drive outflows of HI gas in the ISM. Observations of local starburst galaxies have shown that the presence of outflowing HI gas may be required to avoid complete destruction of the Ly α radiation by dust and to allow its escape from the host galaxies (Kunth et al. 1998; Hayes et al. 2008; Ostlin et al. 2008; Atek et al. 2008). At high redshifts, the Ly α emission line of galaxies is often redshifted relative to other nebular recombination lines (such as H α) and metal absorption lines (e.g. Pettini et al. 2001; Shapley et al. 2003). Furthermore, the spectral shape of the

Ly α emission line is typically asymmetric, with emission extending well into the red wing of the line (e.g. Lequeux et al. 1995). Both of these observations can be explained simultaneously if the observed Ly α photons scatter off neutral hydrogen atoms in an outflowing ‘supershell’ of HI gas that surrounds the star forming regions (Lequeux et al. 1995; Tenorio-Tagle et al. 1999; Ahn et al. 2003; Ahn 2004; Verhamme et al. 2006, 2008). The possibility that Ly α radiation pressure may be important in determining the properties of expanding supershells is exciting, and is discussed in more detail in a companion paper (Dijkstra & Loeb 2008).

Acknowledgments This work is supported by in part by NASA grant NNX08AL43G, by FQXi, and by Harvard University funds. We thank Christian Tapken and an anonymous referee for helpful constructive comments.

REFERENCES

- Abel, T., Norman, M. L., & Madau, P. 1999, *ApJ*, 523, 66
- Abel, T., Bryan, G. L., & Norman, M. L. 2002, *Science*, 295, 93
- Abel, T., Wise, J. H., & Bryan, G. L. 2007, *ApJL*, 659, L87
- Adams, T. F. 1975, *ApJ*, 201, 350
- Ahn, S.-H., & Lee, H.-W. 2002, *Journal of Korean Astronomical*
- Ahn, S.-H., Lee, H.-W., & Lee, H. M. 2003, *MNRAS*, 340, 863
- Ahn, S.-H. 2004, *ApJL*, 601, L25
- Atek, H., Kunth, D., Hayes, M., Ostlin, G., Mas-Hesse, J. M., & . 2008, *ArXiv e-prints*, 805, arXiv:0805.3501
- Barkana, R., & Loeb, A. 2001, *Physics Reports*, 349, 125
- Barkana, R. 2004, *MNRAS*, 347, 59
- Bithell, M. 1990, *MNRAS*, 244, 738
- Bonilha, J. R. M., Ferch, R., Salpeter, E. E., Slater, G., & Noerdlinger, P. D. 1979, *ApJ*, 233, 649
- Castor, J. I., Abbott, D. C., & Klein, R. I., 1975, *ApJ*, 195, 157
- Chandrasekhar, S. 1945, *ApJ*, 102, 402
- Chen, H.-W., Prochaska, J. X., & Gnedin, N. Y. 2007, *ApJL*, 667, L125
- Cox, D. P. 1985, *ApJ*, 288, 465
- Dennison, B., Turner, B. E., & Minter, A. H. 2005, *ApJ*, 633, 309
- Dijkstra, M., Haiman, Z., & Spaans, M. 2006, *ApJ*, 649, 14
- Dijkstra, M., Lidz, A., & Wyithe, J. S. B. 2007, *MNRAS*, 377, 1175
- Dijkstra, M., & Loeb, A. 2008, submitted to *MNRAS*
- Dijkstra, M., et al. 2008, accepted to *MNRAS*
- Elitzur, M., & Ferland, G. J. 1986, *ApJ*, 305, 35
- Furlanetto, S. R., Zaldarriaga, M., & Hernquist, L. 2004, *ApJ*, 613, 1
- Gnedin, N. Y., Kravtsov, A. V., & Chen, H.-W. 2008, *ApJ*, 672, 765
- Haehnelt, M. G. 1995, *MNRAS*, 273, 249
- Haiman, Z., Thoul, A. A., & Loeb, A. 1996, *ApJ*, 464, 523
- Hayes, M., Ostlin, G., Mas-Hesse, J. M., & Kunth, D. 2008, *ArXiv e-prints*, 803, arXiv:0803.1176
- Heger, A., & Woosley, S. E. 2002, *ApJ*, 567, 532
- Heiles, C. 1984, *ApJS*, 55, 585
- Hirata, C. M. 2006, *MNRAS*, 367, 259
- Hui, L., & Gnedin, N. Y. 1997, *MNRAS*, 292, 27

⁷ Continuum radiation may exert a force on steady-state outflows (with a constant mass ejection rate, \dot{M}) around late-type stars that may significantly exceed $\dot{M}\Delta v \gg L_{\text{bol}}/c$ (Salpeter 1974; Ivezić & Elitzur 1995). This is not because of ‘trapping’ of continuum photons, but related to the propagation speed of the photons and the wind. We similarly expect the radiative force of trapped Ly α photons in steady-state outflows to potentially exceed $\dot{M}\Delta v \gg M_F L_\alpha / c$ (and as argued in this paper, it is possible that $M_F L_\alpha / c > L_{\text{bol}}/c$). Note though that these steady-state outflows are clearly different from those discussed in § 3.3, in which a well defined thin shell HI gas is physically separated from the central Ly α source.

Ivezic, Z., & Elitzur, M. 1995, *ApJ*, 445, 415
 Kitayama, T., Yoshida, N., Susa, H., & Umemura, M. 2004, *ApJ*, 613, 631
 Komatsu, E., et al. 2008, *ArXiv e-prints*, 803, arXiv:0803.0547
 Kunth, D., Mas-Hesse, J. M., Terlevich, E., Terlevich, R., Lequeux, J., & Fall, S. M. 1998, *A&A*, 334, 11
 Lee, H.-W., & Ahn, S.-H. 1998, *ApJL*, 504, L61
 Lequeux, J., Kunth, D., Mas-Hesse, J. M., & Sargent, W. L. W. 1995, *A&A*, 301, 18
 Loeb, A., & Rybicki, G. B. 1999, *ApJ*, 524, 527 (LR99)
 Loeb, A. 2001, *ApJL*, 555, L1
 Lucy, L. B. 1999, *A&A*, 344, 282
 Lucy, L. B. 2007, *A&A*, 468, 649
 Maller, A. H., & Bullock, J. S. 2004, *MNRAS*, 355, 694
 McKee, C. F., & Tan, J. C. 2008, *ApJ*, 681, 771
 McClure-Griffiths, N. M., Dickey, J. M., Gaensler, B. M., & Green, A. J. 2002, *ApJ*, 578, 176
 McQuinn, M., Lidz, A., Zahn, O., Dutta, S., Hernquist, L., & Zaldarriaga, M. 2007, *MNRAS*, 377, 1043
 Murray, N., Quataert, E., & Thompson, T. A. 2005, *ApJ*, 618, 569
 Oh, S. P., & Haiman, Z. 2002, *ApJ*, 569, 558
 Osterbrock, D. E. 1989, *Astrophysics of gaseous nebulae and active galactic nuclei*, University of Minnesota, et al. Mill Valley, CA, University Science Books.
 Ostlin, G., Hayes, M., Kunth, D., Mas-Hesse, J. M., Leitherer, C., Petrosian, A., & Atek, H. 2008, *ArXiv e-prints*, 803, arXiv:0803.1174
 Ouchi, M., et al. 2008, *ApJS*, 176, 301
 Partridge, R. B., & Peebles, P. J. E. 1967, *ApJ*, 147, 868
 Pettini, M., Shapley, A. E., Steidel, C. C., Cuby, J.-G., Dickinson, M., Moorwood, A. F. M., Adelberger, K. L., & Giavalisco, M. 2001, *ApJ*, 554, 981
 Pritchard, J. R., & Furlanetto, S. R. 2006, *MNRAS*, 367, 1057
 Pritchard, J. R., & Loeb, A. 2008, *ArXiv e-prints*, 802, arXiv:0802.2102
 Rybicki, G. B., & Lightman, A. P. 1979, *New York, Wiley-Interscience*, 1979. 393 p.,
 Ryder, S. D., Staveley-Smith, L., Malin, D., & Walsh, W. 1995, *AJ*, 109, 1592
 Salpeter, E. E. 1974, *ApJ*, 193, 585
 Schaerer, D. 2002, *A&A*, 382, 28
 Schaerer, D. 2003, *A&A*, 397, 527
 Sethi, S. K., Subrahmanyan, R., & Roshi, D. A. 2007, *ApJ*, 664, 1
 Shapley, A. E., Steidel, C. C., Pettini, M., & Adelberger, K. L. 2003, *ApJ*, 588, 65
 Shimasaku, K., et al. 2006, *PASJ*, 58, 313
 Tapken, C., Appenzeller, I., Noll, S., Richling, S., Heidt, J., Meinköhn, E., & Mehlert, D. 2007, *A&A*, 467, 63
 Tenorio-Tagle, G., & Bodenheimer, P. 1988, *ARA&A*, 26, 145
 Tenorio-Tagle, G., Silich, S. A., Kunth, D., Terlevich, E., & Terlevich, R. 1999, *MNRAS*, 309, 332
 Verhamme, A., Schaerer, D., & Maselli, A. 2006, *A&A*, 460, 397
 Verhamme, A., Schaerer, D., Atek, H., & Tapken, C. 2008, *ArXiv e-prints*, 805, arXiv:0805.3601
 Wyithe, J. S. B., & Loeb, A. 2006, *Nature*, 441, 322
 Yoshida, N., Omukai, K., Hernquist, L., & Abel, T. 2006,

ApJ, 652, 6

APPENDIX A: HI LEVEL POPULATIONS

A1 The (De)Excitation Rates of the 2p Level

Our calculations assumed that all neutral hydrogen atoms populate their electronic ground state (i.e. the 1s level). Below, we explore the physical conditions under which this assumption holds.

Processes that populate the 2p level include: (i) collisional excitation of neutral hydrogen atoms in both the 1s and 2s states by electrons and protons, (ii) recombination into the 2p state following photoionization or collisional ionization, (iii) photoexcitation of 2p level, (iv) photoexcitation of np ($n > 3$) levels, followed by a radiative cascade that passes through the 2p state. Processes that *de-populate* the 2p level include (v) collisional de-excitation to by electrons, (vi) stimulated Ly α emission $2p \rightarrow 1s$ following the absorption of a Ly α photon, and (vii) spontaneous emission of a Ly α photon.

Quantitatively, the rate at which the population in the 2p level is populated is given by

$$\frac{dn_{2p}}{dt} = C_{1s2p}n_en_{1s} + C_{2s2p}n_pn_{2s} + 0.68n_en_{\text{HII}}\alpha_{\text{rec,B}} + (A1)$$

$$\sum_{n=2}^{\infty} P_n n_{1s} f_{n2} - C_{2p1s}n_en_{2p} - C_{2p2s}n_pn_{2p} - P_2n_{2p} - n_{2p}A_{21},$$

where C_{lu} 's denote collisional excitation rate coefficients from level l to u (in $\text{cm}^3 \text{s}^{-1}$), n_x denote number densities of species 'x' (i.e. n_e denotes the electron number density, while n_{HII} denotes the number density of HII ions), P_n denote photoexcitation rates to the state np (in s^{-1}), and f_{n2} denotes the probability that photoexcitation of the np level results in a radiative cascade that passes through the 2p level.

In the reminder of this Appendix, we will estimate the order-of-magnitude of each term.

- The Einstein-A coefficient of the Ly α transition is $A_{21} = 6.25 \times 10^8 \text{ s}^{-1}$. That is, spontaneous emission of Ly α depopulates the 2p state at a rate $A_{21} = 6.25 \times 10^8 \text{ s}^{-1}$.

- Collisional excitation of neutral hydrogen atoms in 1s level by electrons populates the 2p level at a rate $C_{1s2p}n_e = n_e \left[\frac{8.629 \times 10^{-6}}{T^{1/2}} \right] \left[\frac{\Omega(1s,2p)}{g_2} \frac{g_{2p}}{g_{1s}} \right] e^{-\chi/kT} \text{ s}^{-1}$ (e.g. Osterbrock 1989). Here, T denotes the gas temperature in K, n_e is the electron density in cm^{-3} , $g_{1s} = 1$ and $g_{2p} = 3$ are the statistical weights of the 1s and 2p levels, $\Omega(1s,2p) = 0.40 - 0.50$ ($5000 \text{ K} < T < 2 \times 10^4 \text{ K}$, Osterbrock 1989), and $\chi = 10.2 \text{ eV}$ is the energy difference between the 1s and 2p levels. For temperatures $T < 2 \times 10^4 \text{ K}$, we find that $C_{1s2p}n_e < 10^{-10} n_e \text{ s}^{-1}$.

- The collisional excitation rate of neutral hydrogen atoms in 2s level by protons (which dominate over collisions with electrons by about a factor of ~ 10) populates the 2p level at a rate $C_{2s2p}n_p \sim 2 \times 10^{-3} n_p \text{ s}^{-1}$ (e.g. Osterbrock 1989). To assess the term $C_{2s2p}n_p n_{2s}$ requires one to compute n_{2s} . The fraction of atoms in the 2s state is determined by rates similar to those mentioned above, except that the 2s-state is metastable and its Einstein coefficient

is $A_{2s1s} \approx 8 \text{ s}^{-1}$. The 2s-state may therefore be overpopulated relative to the 2p state by orders of magnitude (see e.g. Dennison et al. 2005, and references therein). In close proximity to a luminous source, the 2s level is populated mostly via transitions of the form $1s \xrightarrow{\text{Ly}\beta} 3p \xrightarrow{\text{H}\alpha} 2s$ (Sethi et al. 2007; Dijkstra et al. 2008), and $n_{2s} \sim 0.12 n_{1s} P_3 / A_{2s1s}$, where P_3 is the rate at which Ly β photons are scattered and the prefactor 0.12 denotes the probability that absorption of the Ly β is followed by re-emission of an H α photon (Dijkstra et al. 2008).

- The recombination rate into the 2p level is given by $0.68 \alpha_{\text{rec,B}} n_e n_p = 1.8 \times 10^{-13} (T_{\text{gas}}/10^4 \text{ K})^{-0.7} n_e n_p \text{ cm}^3 \text{ s}^{-1}$ (e.g. Hui & Gnedin 1997), where n_p is the proton density in cm^{-3} .

- The rate at which transitions of the form $1s \rightarrow np$ occur by absorbing a photon is given by $P_n = 4\pi \int \frac{J(\nu)}{h\nu} \sigma_n(\nu) d\nu$. Assuming for simplicity that $J(\nu)$ does not vary with frequency, i.e. $J(\nu) = J$, we have

$$P_n = \frac{4\pi J f_n \pi e^2}{h\nu_n m_e c}, \quad (\text{A2})$$

where f_n denotes the oscillator strength of the transition, e (m_e) the charge (mass) of the electron, and $h\nu_n$ denotes the energy difference between the 1s and np levels. The oscillator strength decreases rapidly with increasing n (e.g. chapter 10.5 of Rybicki & Lightman 1979), and in practice we can safely ignore all terms with $n > 2$. We then need not worry about the factors f_{n2} (which have been computed by Pritchard & Furlanetto 2006; Hirata 2006).

The Ly α scattering rate is given by

$$P_2 = \frac{M_F L_\alpha f_2 \pi e^2}{4\pi r^2 \Delta\nu h\nu_\alpha m_e c}, \quad (\text{A3})$$

where we replaced J (in $\text{erg s}^{-1} \text{ Hz}^{-1} \text{ sr}^{-1} \text{ cm}^{-2}$) with $J = M_F \frac{L_\alpha}{16\pi^2 r^2 \Delta\nu}$, in which L_α is the Ly α luminosity of the central source (in erg s^{-1}), and $\Delta\nu$ is the frequency range over which these Ly α photons have been emitted. The factor M_F takes into account the fact that resonant scattering traps Ly α photons in an optically thick medium (see § 3.3). Substituting fiducial numbers

$$P_2 = 2 \times 10^2 \text{ s}^{-1} \left(\frac{L_\alpha}{10^{42} \text{ erg/s}} \right) \left(\frac{10^{-3} \nu_\alpha}{\Delta\nu} \right) \left(\frac{\text{pc}}{r} \right)^2 \left(\frac{M_F}{100} \right). \quad (\text{A4})$$

The rate at which Ly β photons scatter can be related to the Ly α luminosity, L_α , and the equivalent width (EW) of the line, if one writes the specific intensity $J(\nu_\beta)$ near the Ly β resonance in terms of the Ly α luminosity of the central source as $J(\nu_\beta) = \frac{\lambda_\beta}{\nu_\beta} \frac{L_\alpha}{\text{EW}} \frac{1}{16\pi^2 r^2}$ (note that we assumed that the specific intensity of the continuum remains constant between ν_α and ν_β). The rate at which Ly β photons scatter can then be written as

$$P_3 = 2 \times 10^{-3} \text{ s}^{-1} \left(\frac{L_\alpha}{10^{42} \text{ erg s}^{-1}} \right) \left(\frac{\text{EW}}{200 \text{ \AA}} \right)^{-1} \left(\frac{r}{\text{pc}} \right)^{-2}. \quad (\text{A5})$$

Equation (A5) illustrates that it is very difficult to bring the ratio $n_{2s}/n_{1s} \sim 0.12 P_3 / (A_{2s1s})$ to unity.

- Collisional deexcitation rates relate to the collisional excitation rates via $C_{lu} = C_{ul} \frac{g_u}{g_l} e^{-\chi/kT}$ (e.g. Osterbrock 1989). Combined with the formulas given above, it is straightforward to verify that the collisional de-excitation

rates are subdominant relative to the rate at which spontaneous Ly α emission de-populates the 2p level.

- Lastly, Eq (A4) shows that the stimulated emission rate is $P_2 \ll A_{21}$.

A2 HI Level Populations in this Paper

The maximum number density of hydrogen nuclei in this paper is encountered in § 3.3, for the expanding shell of HI gas with $N_{\text{HI}} = 10^{21} \text{ cm}^{-2}$ and a thickness $dr = 0.01 \text{ kpc}$, in which $n_{\text{max}} \sim 30 \text{ cm}^{-3}$. At these column densities, the shell self-shields against ionizing radiation, and is likely mostly neutral. For simplicity, let us assume that $n_e = n_p = n_{\text{HI}} = 30 \text{ cm}^{-3}$. Under these conditions:

- the collisional excitation rate from $1s \rightarrow 2p$ is $C_{12} < 3 \times 10^{-9} \text{ s}^{-1}$.

- the collisional excitation rate from $2s \rightarrow 2p$ per atom in the 1s state- is $C_{2s2p} n_{2s} n_p / n_{1s} \sim 5 \times 10^{-2} n_{2s} / n_{1s} \text{ s}^{-1} = 5 \times 10^{-3} P_3 / A_{2s1s} \text{ s}^{-1}$. The maximum Ly α luminosity considered in this paper is $\sim 10^{43} \text{ erg s}^{-1}$. Let us conservatively assume that $\text{EW} = 20 \text{ \AA}$ (rest-frame), which corresponds roughly to the detection threshold that exists in narrow-band surveys (e.g. Shimasaku et al. 2006). Using Eq A5, we find that $P_{3,\text{max}} \sim 10^{-5} \text{ s}^{-1}$ (for $r = 0.1 \text{ kpc}$), and therefore that $C_{2s2p} n_{2s} n_p / n_{1s} \sim 10^{-8} \text{ s}^{-1}$.

- the recombination rate is $5 \times 10^{-12} (T_{\text{gas}}/10^4 \text{ K})^{-0.7} \text{ s}^{-1}$.
- the maximum Ly α scattering rate is (substituting $r = 0.1 \text{ kpc}$, $M_F = 100$, $\Delta\nu = 0.001 \nu_\alpha$ into Eq A4) $P_{2,\text{max}} = 0.2 \text{ s}^{-1}$.

By comparing these rates to the rate at which spontaneous emission of Ly α depopulates the 2p state, $A_{21} = 6.25 \times 10^8 \text{ s}^{-1}$, we find that all excitation rates are ≥ 9 orders of magnitude smaller than the de-excitation rate for the wind models discussed in § 3.3. In equilibrium, hydrogen atoms in their electronic ground (1s) state are therefore ≥ 9 orders of magnitude more abundant than hydrogen atoms in their first excited (2p) state. Furthermore, as was mentioned above the ratio of atoms in the 2s and 1s levels is given by $n_{2s}/n_{1s} = 0.12 P_{3,\text{max}} / A_{2s1s} \sim 10^{-7}$. Since the densities, Ly α luminosities, and the Ly β scattering rates are lower, the fraction of HI atoms in their first excited states are even smaller in other sections of the paper. In conclusion, for all applications presented in this paper, no accuracy is lost by assuming that all hydrogen atoms occupy their electronic ground state.

Finally, in 2.2 we computed solutions for the radial dependence of $U(r)$ (Fig 1). The energy density, $U(r)$, was quoted to depend linearly on the luminosity of the central source. This is valid unless (i) the Ly α scattering rate, $P_2 > A_{21} = 6.25 \times 10^8 \text{ s}^{-1}$, or (ii) the Ly β scattering rate exceeds $P_3 \gtrsim 10^2 \text{ s}^{-1}$. In either case, our assumption that all hydrogen atoms populate their electronic ground state breaks down. Condition (i) translates to $L_\alpha \gtrsim 3 \times 10^{48} \text{ erg s}^{-1} (\Delta\nu/0.001\nu_\alpha)(r/\text{pc})^2 (100/M_F)$ (Eq. A4), while condition (ii) translates to $L_\alpha \gtrsim 10^{46} \text{ erg s}^{-1} (\text{EW}/20 \text{ \AA})(r/\text{pc})^2$ (Eq. A5). Substituting $r = 0.1 \text{ kpc}$, $M_F = 100$ (Fig 1 shows that resonant scattering enhances the energy density by a factor of $\gtrsim 10$ relative to $L_\alpha/4\pi r^2 c$), $\Delta\nu = 10^{-3} \nu_\alpha$ (thermal broadening alone in $T = 10^4 \text{ K}$ gas results in $\Delta\nu \sim 26 \text{ km s}^{-1}$, which translates to $\Delta\nu = 10^{-4} \nu_\alpha$), and $\text{EW} = 20 \text{ \AA}$,

condition (i) translates to $L_\alpha \gtrsim 3 \times 10^{52} \text{ erg s}^{-1}$, while condition (ii) translates to $L_\alpha \gtrsim 10^{50} \text{ erg s}^{-1}$. The more conservative condition (ii), $L_\alpha \gtrsim 10^{50} \text{ erg s}^{-1}$, translates to $\dot{N}_{54} \gtrsim 10^7$, well beyond the regime considered in this paper.